J|A|C|S
ARTICLES
Published on Web 03/11/2004

NMR-Based Characterization of Phenothiazines as a RNA Binding Scaffold†

Moriz Mayer and Thomas L. James*

Contribution from the Department of Pharmaceutical Chemistry, 600 16th Street-Mission Bay, University of California, San Francisco, California 94143-2280

Received December 1, 2003; E-mail: james@picasso.ucsf.edu

Abstract: Phenothiazines were identified by virtual screening as promising ligands for HIV-1 TAR RNA and A-site ribosomal RNA, and binding in each case was verified experimentally. Consequently, since phenothiazines generally possess high bioavailability and low toxicity, we used several NMR techniques to explore the binding characteristics of acetopromazine with a total of five different RNA constructs: four as potential drug targets plus one control RNA construct. Acetopromazine was able to bind to various internal bulges and terminal loops containing both purines and pyrimidines, but no binding could be detected with double-stranded RNA or tetraloops. Dissociation constants determined via NMR varied from 0.27 to >3 mM. Analysis of differential saturation transfer difference (STD) NMR effects of acetopromazine suggests that the phenothiazine moiety has the closest contact to the binding sites of TAR and A-site RNA while the flexible *N*,*N*-dimethylpropylamino side chain contributes less to binding. NMR studies on A-site ribosomal RNA binding by six commercially available phenothiazines, while too few to establish a true structure−activity relationship, revealed a distinct dependence on aromatic ring and side chain substituents. Substituted phenothiazines have low molecular weight, are not highly charged, and have an inherent affinity for irregular tertiary RNA folds, suggesting that they can serve as a novel scaffold for constructing RNA-binding ligands.

Introduction

RNA is becoming a valuable target for drug discovery.[1,2] Regions of RNA folding into complex tertiary structures are particularly interesting since they play important roles in RNA−RNA and protein−RNA interactions as exemplified in the ribosome. These interactions are crucial for a variety of cellular processes including transcription, translation, and the control of gene expression.[3,4] Therefore, targeting RNA can provide the means to fight diseases which are otherwise difficult or impossible to address such as viral diseases or with disorders where protein targets posit problems, e.g., with bacterial multidrug resistance.[5] Discovery of small, druglike molecules that bind specifically to unique tertiary RNA folds consequently have a vast potential.[6]

Current drugs inhibiting specific RNA functions such as aminoglycosides, oligopeptides, and their derivatives are far from optimal in regard to their pharmacokinetic properties.[7] Another major disadvantage of many known RNA-binding molecules is that their multiple positive charges render them nonspecific at higher concentrations.[8] While high affinity interactions in the nanomolar range are readily attainable with aminoglycosides and their derivatives, site specificity still poses a major challenge in targeting RNA.[9] Also, they can usually not be regarded as small molecules because their molecular weight is above the drug designer's ideal threshold of 500 Da.[10] RNA intercalators are typically less polar while retaining high affinity, but they typically possess high molecular weight and lack specificity for discrete tertiary structures.[9,11] It would therefore be extremely valuable to have a scaffold with an inherent affinity toward RNA without the negative effects of high molecular weight and high polarity. Fine-tuning of a druglike scaffold can eventually lead to molecules with high affinity for a specific RNA motif as well as good druglike properties.

Phenothiazines consist of a nonplanar heterotricyclic ring system in which two benzene rings are fused to a 1,4-diheterosubstituted benzene. The nonplanar structure of the molecule prevents it from binding to nucleic acids solely by intercalation. N-substituted derivatives of this scaffold such as chlorpromazine (thorazine) and trifluorperazine (stelazine) have been in clinical use for many years to treat mental

† Abbreviations: A-site, aminoacyl-tRNA site; NOESY, nuclear Overhauser and exchange spectroscopy; trNOESY, transferred NOESY; STD, saturation transfer difference; TAR RNA, trans-activating response element RNA; TOCSY, total correlation spectroscopy; SAR, structure−activity relationship.

(1) Hermann, T.; Westhof, E. *Curr. Opin. Biotechnol.* **1998**, *9*, 66−73.
(2) Tor, Y. *Chembiochem* **2003**, *4*, 998−1007.
(3) Cheng, A. C.; Calabro, V.; Frankel, A. D. *Curr. Opin. Struct. Biol.* **2001**, *11*, 478−484.
(4) Hwang, S.; Tamilarasu, N.; Ryan, K.; Huq, I.; Richter, S.; Still, W. C.; Rana, T. M. *Proc. Natl. Acad. Sci. U.S.A.* **1999**, *96*, 12997−13002.
(5) Vicens, Q.; Westhof, E. *Chembiochem* **2003**, *4*, 1018−1023.
(6) Hermann, T. *Biopolymers* **2003**, *70*, 4−18.
(7) Mei, H.-Y.; Mack, D. P.; Galan, A. A.; Halim, N. S.; Heldsinger, A.; Loo, J. A.; Moreland, D. W.; Sannes-Lowery, K. A.; Sharmeen, L.; Truong, H. N.; Czarnik, A. W. *Bioorg. Med. Chem.* **1997**, *5*, 1173−1184.
(8) Sannes-Lowery, K. A.; Griffey, R. H.; Hofstadler, S. A. *Anal. Biochem.* **2000**, *280*, 264−271.
(9) Luedtke, N. W.; Liu, Q.; Tor, Y. *Biochemistry* **2003**, *42*, 11391−11403.
(10) Lipinski, C. A.; Lombardo, F.; Dominy, B. W.; Feeney, P. J. *Adv. Drug Delivery Rev.* **2001**, *46*, 3−26.
(11) Carlson, C. B.; Vuyisich, M.; Gooch, B. D.; Beal, P. A. *Chem. Biol.* **2003**, *10*, 663−672.

disorders such as schizophrenia, paranoia, and psychosis. This also means that these compounds have been thoroughly tested for toxicity and that they have good pharmacokinetic properties since they can cross the blood brain barrier. Recently these compounds were back in the headlines because clinical trials were performed to test their effectiveness in treating patients with the new variant Creutzfeldt−Jacob disease (nvCJD).[12,13] Phenothiazines have also been studied with regard to their antimicrobial properties, and their use has been proposed to fight multidrug-resistant bacteria.[14,15] Last year this laboratory published a paper showing that phenothiazines bind to trans-activation response element (TAR) RNA of HIV-1 and inhibit the interaction with Tat protein, which is an essential step in the viral replication cycle.[16] The structure of the HIV-1 TAR RNA−acetopromazine complex was subsequently solved by NMR spectroscopy.[17]

In this study, we use NMR to examine the binding propensity of phenothiazines for other RNA structural elements. Some, but not all, RNA structural elements bind phenothiazines. The phenothiazines exhibited different preferences for binding to the various RNA elements.

Methods and Materials

Preparation of RNA Samples. Unlabeled RNA samples were obtained by in vitro transcription using T7 RNA polymerase and a synthetic DNA template[18] The DNA templates consisted of a double-stranded 18-base pair T7 promoter sequence and a single-stranded coding sequence. The transcription buffer contained 80 mM Tris (pH 8.1), 10 mM dithiothreitol, 1 mM spermidine, 300 nM template DNA, and $MgCl_2$, NTPs, and T7 RNA polymerase in varying concentrations optimized for the respective RNA molecules. Transcription reactions were incubated overnight at 37°C. RNAs were precipitated by adding 10% (v/v) of a 5 M NaCl solution and three volumes of ethanol. Precipitated RNA was redissolved in 8 M urea after drying. The desired RNA was then separated on 20% (w/v) 19:1 polyacrylamide gels containing 8 M urea. The RNA band was visualized by UV shadowing and excised from the gel; the RNA was extracted by electroelution using an Elutrap apparatus from Schleicher & Schuell. The RNA was subjected to three ethanol precipitations and then desalted by passing it through a Sephadex G25 gel filtration column. Purified RNAs were resuspended in NMR buffer that contained 20 mM sodium phosphate (pH 6.8) and 50 mM sodium chloride. Samples were dissolved in 99.9% D_2O after lyophilization. RNA solutions were heated to 90°C and snap cooled in an ice bath in the NMR tube for annealing. Final RNA concentrations were 50 μM for the STD experiments, 100−200 μM for the TOCSY experiments, and ca. 700 μM for the NOESY experiment. Reagents and phenothiazine derivatives were purchased from Sigma.

NMR Spectroscopy. NMR experiments were performed on either a Varian Inova 600 MHz or a Bruker DRX 500 MHz spectrometer equipped with a cryoprobe. All STD experiments were acquired on the 600 MHz spectrometer with internal subtraction by phase cycling.[19] On-resonance irradiation was set to 5.5 ppm, and off-resonance irradiation was set to ca. 30 ppm where no RNA resonances were present. Typically, 256 scans were acquired for the STD experiments. Presaturation of RNA resonances was achieved by a band-selective G4 Gaussian cascade pulse. To test the shaped pulse selectivity, a STD experiment on acetopromazine alone without RNA present was acquired. No ligand signals were present in the STD spectrum, proving the selectivity of the G4 pulse. In saturation time experiments, the total recycle delay time was kept constant and curve fitting of the data was performed with Kaleidagraph Version 3.52 on a Macintosh computer. Temperature was set to 15 °C in all STD experiments. Most 1D STD NMR spectra were analyzed on Xwinnmr 3.0 Bruker software. Varian spectra were converted in to Bruker format accordingly. 1D NMR imino spectra were acquired with hard pulse WATERGATE water suppression, with the excitation profile optimized for maximum intensity at 13 ppm. The T1 experiment on the 20:1 acetopromazine−RNA sample was acquired with the inversion recovery pulse sequence and processed and analyzed with vnmr 6.1C software. 2D spectra were processed with NMRPipe/NMRDraw[20] and analyzed with SPARKY.[21] In the 2D homonuclear experiments, the States-TPPI method was used to achieve quadrature detection in the indirect dimensions. Homonuclear 2D TOCSY and NOESY spectra were recorded in D_2O at 15 or 25 °C with a relaxation delay of 1.5 s. The spectral width was set to 6000 Hz in both dimensions. Mixing times of 200−300 ms and a spin lock time of 50 ms were used for the NOESY and TOCSY spectra, respectively. A total of 256 FIDs and 2048 complex data points were collected. The residual HDO resonance was suppressed by a low power presaturation pulse during the relaxation delay.

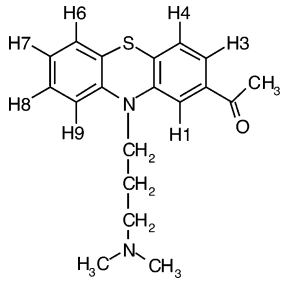

Figure 1. Structure and nomenclature of acetopromazine.

Results and Discussion

Acetopromazine Binding to A-Site RNA. A structure-based in-silico screening of the Available Chemicals Directory (ACD) against the NMR structure[22] of the 16 S aminoacyl-tRNA site (A-site) of ribosomal RNA (1pbr) showed an enrichment of phenothiazine derivatives in the high ranking compounds. We chose acetopromazine (Figure 1) as our initial test molecule because of its high solubility in aqueous solution. Initial binding tests by 1D STD NMR spectra[23,24] proved that acetopromazine binds to the 27mer model A-site RNA we used in these experiments. Figure 2A shows the reference NMR spectrum of a mixture of acetopromazine and A-site RNA, and B shows the STD NMR spectrum with a saturation time of 0.3 s. Spectrum C was acquired with parameters identical with those of spectrum B but with a saturation time of 3 s. All resonances upfield from 4 ppm belong to the ligand so they are easily distinguishable from RNA signals. Even the aromatic protons of acetopromazine can be observed readily due to the 20-fold

(12) Amaral, L.; Kristiansen, J. E. *Int. J. Antimicrob. Agents* **2001**, *18*, 411−417.
(13) Korth, C.; May, B. C.; Cohen, F. E.; Prusiner, S. B. *Proc. Natl. Acad. Sci. U.S.A.* **2001**, *98*, 9836−9841.
(14) Mazumder, R.; Ganguly, K.; Dastidar, S. G.; Chakrabarty, A. N. *Int. J. Antimicrob. Agents* **2001**, *18*, 403−406.
(15) Kristiansen, J. E.; Mortensen, I. *Pharmacol. Toxicol.* **1987**, *60*, 100−103.
(16) Lind, K. E.; Du, Z.; Fujinaga, K.; Peterlin, B. M.; James, T. L. *Chem. Biol.* **2002**, *9*, 185−193.
(17) Du, Z.; Lind, K. E.; James, T. L. *Chem. Biol.* **2002**, *9*, 707−712.
(18) Milligan, J. F.; Uhlenbeck, O. C. In *Methods in Enzymology*; Dahlberg, J. E., Abelson, J. N., Eds.; Academic Press: New York, 1989; Vol. 180, pp 51−62.
(19) Mayer, M.; Meyer, B. *J. Am. Chem. Soc.* **2001**, *123*, 6108−6117.
(20) Delaglio, F.; Grzesiek, S.; Vuister, G. W.; Zhu, G.; Pfeifer, J.; Bax, A. *J. Biomol. NMR* **1995**, *6*, 277−293.
(21) Goddard, T. D.; Kneller, D. G. *Sparky*, 3.0 ed.; University of California: San Francisco, CA, 1998.
(22) Fourmy, D.; Recht, M. I.; Blanchard, S. C.; Puglisi, J. D. *Science* **1996**, *274*, 1367−1371.
(23) Mayer, M.; Meyer, B. *Angew. Chem., Int. Ed.* **1999**, *38*, 1784−1788.
(24) Mayer, M.; James, T. L. *J. Am. Chem. Soc.* **2002**, *124*, 13376−13377.

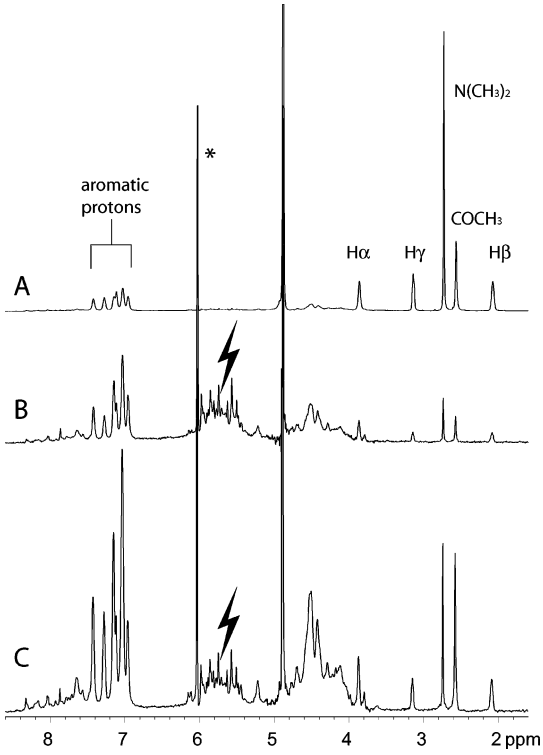

Figure 2. (A) Reference NMR spectrum of a mixture of 2 mM acetopromazine and 0.1 mM of the 27mer model of A-site RNA. The asterisk demarks the maleate salt contained in the purchased acetopromazine. (B) STD NMR spectrum of the mixture with on-resonance irradiation at 5.5 ppm as indicated by the arrow and a saturation time of 0.3 s. (C) STD NMR spectrum identical with (B) but with a saturation time of 3 s. There is a large increase in STD signal intensity from spectrum B to C. One can also observe the differential STD effects used for mapping the ligand epitope (cf. Table 1).

excess of the drug. Ligand signals appearing in the STD spectra are due to the transfer of saturation to the drug from the RNA while in the bound state. Therefore, any signals from small molecules in the STD experiment prove their binding interaction with the RNA. In addition, the differential STD signals permit characterization of the binding epitope of the ligand.[19]

The size of the observed STD signal is dependent not only on proximity to the receptor, however. Saturation of ligand protons in the bound state is counteracted by their longitudinal relaxation times T1 in the free state.[23] It is possible to misinterpret a large STD effect at long saturation times for a strong contact if no T1 measurements or STD build-up curves are acquired. Therefore, it is important to take this effect into account for molecules that have protons differing substantially in their T1 values. Short presaturation times of the macromolecule should be more accurate for epitope mapping experiments, because the T1 effect has a smaller impact.[25,26] Acetopromazine at a 20:1 ligand-to-RNA ratio has T1 times ranging from 0.39 s for the Hα protons to 1.88 s for the H4/H7 protons on the aromatic ring. We normalized the STD signal of the H6 proton of the ligand to 100 at saturation times of 0.3 and 3 s for ease of comparison (Table 1). The largest STD effects can be observed for the H6 and H4/H7 protons of the aromatic ring systems at both saturation times. However, for some protons we did observe considerable changes in the STD intensities when the saturation time was reduced to 0.3 s. For example the H1 and H9 proton STD intensities increased by 23% and 50%, respectively, while the methyl proton STD intensity of the acetyl group decreased by 77%. Clearly, this can be attributed to the different T1 relaxation times. The T1 values of the H1 and H9 protons are 0.8 and 0.67 s, respectively, whereas the T1 value for the acetyl group methyl protons is 1.53 s. The general trend is that protons with short T1 times increase their relative STD intensities when shorter saturation times are used for analysis, while the STD intensities for protons with long T1 times decrease accordingly.

While the overall binding characteristics of the ligand's epitope remains largely the same at 0.3 or 3 s saturation times, we propose the use of STD build-up curves to prevent possible misinterpretations. Figure 3 shows the STD build-up curves of three ligand groups. Here, the STD amplification factors[19,26] are plotted against the saturation time. To eliminate the T1 bias at long saturation times, the slope of the STD build-up curve at a saturation time of 0 was obtained by fitting the saturation time data to the monoexponential equation: $STD = STD_{max}(1 - e^{(-k_{sat}t)})$, where STD stands for the STD signal intensity of a given proton at saturation time t, STD_{max} is the maximal STD intensity obtainable when long saturation times are used, and k_{sat} stands for the observed saturation rate constant. Multiplica-

Table 1. STD Signal Intensities of Acetopromazine at 0.3 and 3 s Saturation Time As Determined from the Spectra in Figure 2[a]

	STD (0.3 s)	STD (3 s)	STD (fit)	T1 (s)
H1	49	40	55	0.8
H3	80	78	77	1.76
H4/H7	86	92	86	1.88
H6	100	100	100	1.84
H8	57	60	53	1.36
H9	77	51	94	0.67
$COCH_3$	11	19	9	1.53
Hα	21	15	24	0.39
Hβ	14	9	15	0.45
Hγ	11	7	11	0.55
$N(CH_3)_2$	4	5	3	0.77

[a] STD (fit) corresponds to the STD intensity as calculated from fitting the data to an exponential equation (Figure 3). For ease of comparison, the STD effects were normalized to the H6 aromatic signal, which was set to 100. The respective T1 relaxation times of the ligand at the 20:1 excess are also displayed.

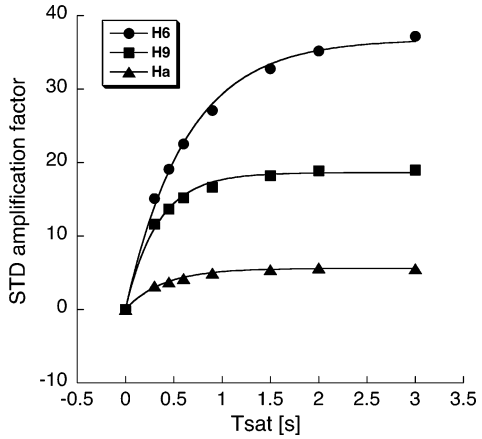

Figure 3. STD build-up curves for three acetylpromazine protons with different T1 times. The circle corresponds to the H6 aromatic proton with a T1 time of 1.84 s, the square corresponds to the H9 protons with a T1 time of 0.67 s, and the triangle corresponds to the Hα protons with a T1 time of 0.39 s. Experimental data were fit to a rising exponential to obtain STD_{max} and the saturation rate constant k_{sat}.

(25) Jayalakshmi, V.; Krishna, N. R. *J. Magn. Reson.* **2002**, *155*, 106−118.
(26) Yan, J.; Kline, A. D.; Mo, H.; Shapiro, M. J.; Zartler, E. R. *J. Magn. Reson.* **2003**, *163*, 270−276.

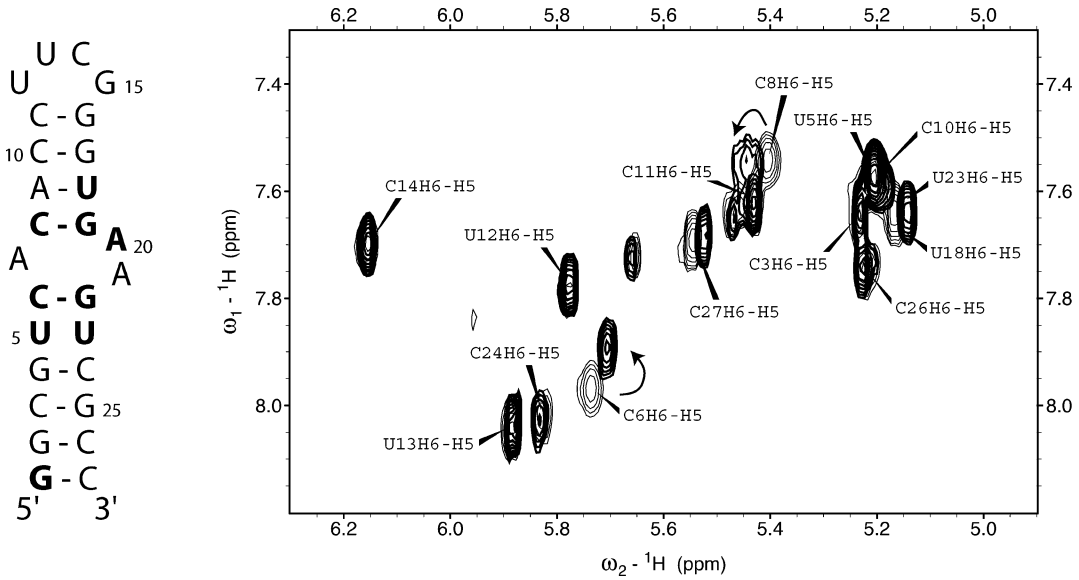

Figure 4. Sequence of the 27 mer A-site RNA. Residues where at least one proton resonance shifts by more than 0.03 ppm as determined from 2D TOCSY and NOESY spectra are marked in bold. The overlaid TOCSY spectra of free RNA (thin lines) and a 1:1 complex of 0.7 mM RNA and acetopromazine (thick lines) of the pyrimidine H5, H6 proton region are also shown. The residues with the largest shifts are the H5, H6 protons of residues C6 and C8, which are adjacent to the asymmetric internal loop. This also provides evidence that the interaction of the drug is specific to the internal bulge region.

tion of the observed saturation rate constant k_{sat} and the maximal STD intensity STD_{max} yields the slope of the curve at zero saturation time. This slope corresponds to the STD intensity in the absence of T1 bias. To compare the STD values obtained by this analysis with the previous data interpretations, we again normalized the intensities by referencing to the resonance with the largest STD effect, H6. The relative values obtained are displayed in Table 1. They agree well with the STD intensities obtained at the short saturation time of 0.3 s. An advantage of curve fitting is that it eliminates the need of obtaining T1 data for protons at various ligand-to-receptor ratios; it also gives better results than STD data obtained at a single short saturation time, which will often suffer from a poor signal-to-noise ratio. Therefore, the slope value should more accurately reflect the proximity of ligand protons to receptor protons.

STD intensities within the aromatic ring vary between 53 and 100; the H1 and H8 protons show the weakest and the H6 and H9 protons show the strongest STD effects. The acetyl methyl protons manifest a substantial intensity decrease compared to the ring protons, and STD intensities within the aliphatic chain also decrease continuously with increasing distance from the ring protons. The smallest STD effects are observed for the two methyl groups of the aliphatic chain. In summary, the largest STD effects are observed for the tricyclic ring system, which implies that the aromatic groups of the acetopromazine have the closest contact to the A-site RNA while the aliphatic side chain interacts less strongly. This is especially true for the Hγ protons and the *N*-methyl groups which have the smallest STD intensities.

To further characterize the contact area of the ligand with A-site RNA, we performed 2D TOCSY and NOESY experiments noting which proton resonances experienced chemical shifts upon addition of the ligand. The 2D TOCSY experiments provided a fast and easy way to follow shifts of the H5−H6 protons of the pyrimidine bases. Since it is a very sensitive NMR technique, only small amounts of RNA are needed and the time required is minimal. We used ca. 100−200 μM RNA and obtained spectra with good signal-to-noise ratio within 2 h on a 600 MHz spectrometer. The disadvantage is that only the H5−H6 protons of the pyrimidines can be monitored because the ribose ring protons are too overlapped. Not even the relatively dispersed anomeric protons can be used because the predominant 3′-endo conformation of the ribose in RNA results in a small H1′−H2′ coupling constant. Cross-peaks from the anomeric proton region to the ribose ring protons of RNA are therefore not detectable in the TOCSY experiment.

Figure 4 shows the secondary structure of the model 27mer A-site RNA and the overlaid TOCSY spectra of the H5, H6 pyrimidine spectral region of the A-site RNA in the presence and absence of acetopromazine. The largest shifts are observed for the C6 and C8 residues. Smaller shifts can be observed for U18, the wobble U5−U23 base pair, and C27 of the closing base pair. Significant shifts are only observed for resonances located close to the asymmetric bulge formed by the three adenosine nucleotides A7, A20, and A21.

Because cross-peaks of the aromatic purine protons are not observable in the TOCSY spectrum, we performed a NOESY experiment to monitor shifts of the adenosine base protons. Interestingly, only the H2 and H8 resonances of the A20 showed a considerable shift, i.e., above the chosen threshold of 0.03 ppm. Neither A7 nor A21 aromatic proton resonances shifted much upon addition of acetopromazine. A small change in chemical shift upon addition of ligand was observed for the closing bases G1 and C27. This could be an indication of the aromatic rings stacking onto the closing base pairs or the additional flexibility of this part of the RNA accommodating the drug or the positively charged drug interacting nonspecifically with the triphosphate of G1.

The well-resolved imino region provides an additional means to identify binding interactions as well as determination of the binding affinity.[27] Figure 5 shows stacked 1D NMR spectra of the imino resonance region of 100 μM A-site RNA that were acquired with increasing amounts of acetopromazine. By

(27) Yu, L.; Oost, T. K.; Schkeryantz, J. M.; Yang, J.; Janowick, D.; Fesik, S. W. *J. Am. Chem. Soc.* **2003**, *125*, 4444−4450.

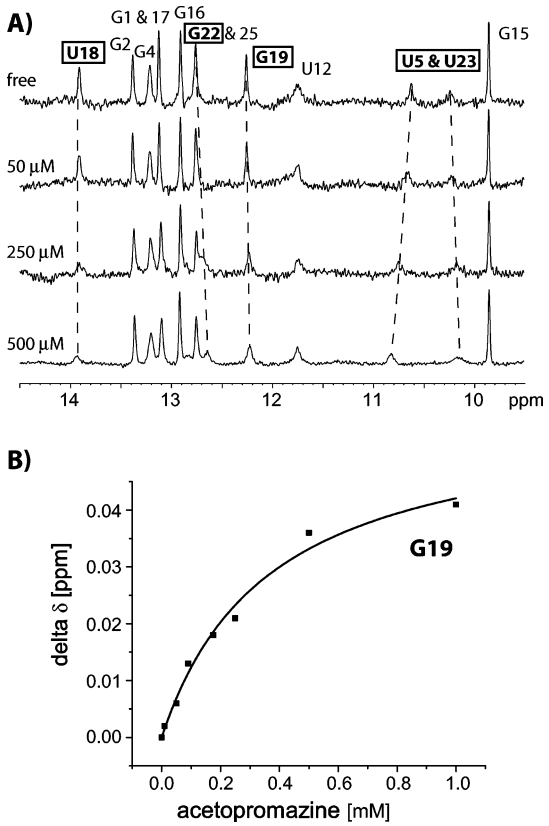

Figure 5. Stacked plot of 1D NMR spectra of the imino region of 100 μM A-site RNA with increasing concentrations of acetopromazine from free RNA in the top spectrum to 500 μM in the bottom spectrum. Boxed residues indicate broadened and/or shifted imino resonances. Only imino resonances that are adjacent to the internal bulge shift upon addition of acetopromazine (cf. Figure 4). The dissociation constant of 0.37 $\pm$ 0.06 mM was determined by fitting the imino resonance chemical shift of G19 to a one-site binding curve as displayed in the plot on the bottom.

monitoring the chemical shift changes of the imino resonances upon titration of acetopromazine, it is possible to do two things: (a) determine the binding site; (b) calculate the dissociation constant K_D. In agreement with the TOCSY spectra, resonances shifted and/or broadened are those adjacent to the asymmetric internal bulge. The imino resonances experiencing changes are those of U18, G19, G22, and the wobble U5, U23 pair. By plotting the chemical shift changes as a function of ligand concentration as shown in Figure 5, it is possible to calculate the K_D value. Figure 5 shows how the chemical shift of resonance G19 moves upfield upon addition of acetopromazine as well as the curve obtained from fitting the data to a simple one-site binding equation. The calculated K_D value was 370 μM, which corresponds to a weak affinity interaction. The G19 signal was the only imino resonance we could use for an accurate calculation of the K_D value. For the other resonances experiencing changes upon titration of acetopromazine, either the chemical shift difference was not large enough (U18), they were overlapped (G22), or they exchange broadened to such an extent that their signals were no longer observable at acetopromazine concentrations above 500 μM (U5 and U23).

The NOESY spectrum gave an additional indication of binding because large transferred NOEs were observed for the ligand (not shown).[28] NOE cross-peaks of a small ligand have the opposite sign compared to the diagonal when free in solution,

(28) Meyer, B.; Weimar, T.; Peters, T. *Eur. J. Biochem.* **1997**, *246*, 705−709.

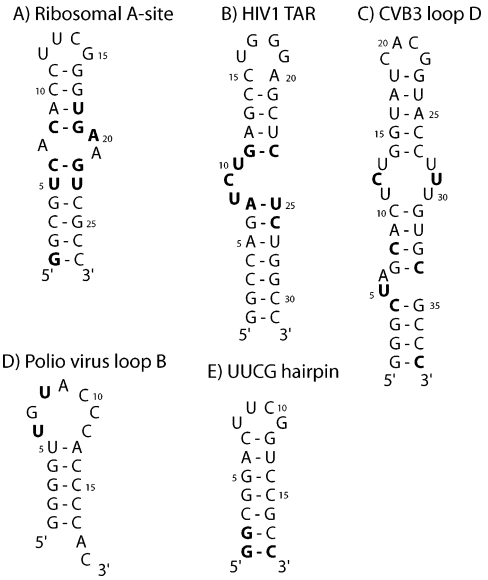

Figure 6. Secondary structure of five RNA molecules that were tested for their interaction with acetopromazine ranging from 18 to 38 residues in length (cf. text). The residues marked in bold showed a chemical shift difference of greater than 0.03 ppm at acetopromazine concentrations ranging from 0.5 to 0.7 mM depending on the RNA. Only chemical shifts of the H5, H6 pyrimidine base protons were monitored for structures C and D; for the other three structures 2D NOESY spectra were also collected.

due to a small molecule's rapid molecular tumbling rate. In the case of reversible interaction with the large RNA molecule, as observed here, the average tumbling time of the ligand increases and the sign of the ligand's NOE signals change from positive to negative giving them the same sign as the diagonal. Therefore, the change in sign of the ligand's NOEs is evidence of binding. Presumably due to the low binding affinity, only two very weak intermolecular NOEs between the ligand and the RNA were observed. The cross-peaks were between the RNA's A7 H8 proton and the methyl protons of the acetyl group of acetopromazine and the RNA's A21 H2 proton and the Hγ protons of the acetopromazine side chain. From the epitope mapping experiment we learned that the aromatic protons are in closer contact to the RNA than the Hγ and methyl protons of the aliphatic side chain. However, no intermolecular NOEs between any of the aromatic protons, which exhibit the largest STD effects, and the RNA are observable at a mixing time of 250 ms and 0.7 mM 1:1 RNA−ligand concentration. A possible explanation could be that the severe line broadening of the aromatic ring protons leads to intermolecular NOEs that are broadened and consequently are difficult to distinguish above the noise level.

Acetopromazine Binding to Other RNA Structures. Our laboratory has previously studied the TAR RNA complex formed with acetopromazine. The HIV-1 TAR RNA construct consists of a 31mer containing an asymmetric pyrimidine-rich UCU bulge. As reported, acetopromazine binds exclusively to the asymmetric bulge of TAR RNA. Signals shifting upon addition of acetopromazine are indicated by bold characters in Figure 6B. Gel shift assays and a cell-based Tat transactivation assay performed with TAR RNA and the ligand acetopromazine demonstrated inhibition of the Tat-TAR binding with the interaction manifesting high affinity in the low micromolar to high nanomolar range.[16] The large number of intermolecular NOEs obtained from the complex was also indicative of a higher

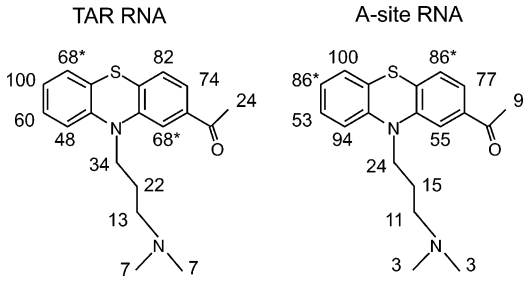

Figure 7. Comparison of the epitope mapping results of the acetopromazine bound to TAR RNA and A-site RNA. The concentration of the RNA was 100 μM, and a 20-fold excess of acetopromazine was used in both experiments. Values marked with an asterisk correspond to overlapped signals which could not be analyzed separately.

affinity interaction.[17] However the imino and TOCSY chemical shift monitoring experiment performed in the current study resulted in a much higher dissociation constant of 270 μM. It remains unclear why both the gel shift assays and the cell-based assays yielded results that differed so much from the NMR titrations performed here. Although unlikely, a possibility that needs to be tested is that the strong inhibitory effect of acetopromazine was due to the interaction with the Tat protein instead of the TAR RNA in the above-mentioned experiments. However, under the NMR experimental conditions used in this study, we do ascertain the weak affinity interaction. It is in fact more common to detect weak ligands from virtual screening runs, and the discovery of a sub-micromolar "hit" can usually not be expected.

Figure 7 compares the epitope mapping of acetopromazine to A-site RNA and TAR RNA binding site at a 20:1 ligand excess. As for the A-site, the STD intensities for the TAR RNA were obtained from fitting the saturation time data to the rising exponential equation. For TAR RNA binding, the overall differences in the aromatic ring system are not as pronounced with differential STD effects ranging from 62 to 100 compared with effects ranging from 53 to 100 in the A-site RNA. In both cases, there is a large decrease in STD intensity along the aliphatic side chain with the two methyl groups having a STD value of only 7 in the case of TAR RNA. The STD analysis implies that the aromatic rings of the ligand make good contact with the TAR RNA binding site but the acetyl and aliphatic moieties are not bound as tightly. If we compare the STD results with the NMR structure of the complex,[16] there is good agreement for the aromatic part of acetopromazine. The low STD enhancement of the acetyl group also agrees with the structure, since it essentially points out of the binding pocket and has a relative STD value of only 24. In the NMR structure, the aliphatic side chain of acetopromazine fits tightly into the minor groove of the RNA with multiple intermolecular proton−proton contacts at distances between 2.6 and 4 Å. However, the low STD effects ranging from 7 to 34 do not reflect this. A possible explanation for this observation could be the flexibility of the side chain. Since the NMR structure represents the time-averaged structure of the reversible binding interaction, the side chain may be completely inserted into the minor groove for only a fraction of the bound structures. An unrestrained molecular dynamics simulation of this complex showed fluctuation of the propylamino side chain in and outside of the binding pocket while the tricyclic ring system remained fixed in the binding site (T. Downing, unpublished results). With the side chain being bound part of the time, NOE contacts can be observed that will result in the side chain being placed inside the minor groove in the refined NMR structure. In reality this conformation is likely to be populated only part of the time resulting in lower STD effects.

Overall the binding modes of acetopromazine toward the two RNA structures show some general similarities. The largest STD effects come from the tricyclic ring system, and the aliphatic chain does not appear to interact as extensively, the two *N*-methyl groups furthest away from the aromatic groups having the weakest interaction. Nevertheless, there are some important differences showing that the mapping is in effect responsive to the individual binding orientations. Most notably, the H9 proton of acetopromazine bound to the A-site has one of the highest relative STD effects, while in the TAR RNA this proton has the lowest STD effect of the aromatic protons. Regarding the direction of compound optimization, one can conclude from the epitope mapping experiments that the aliphatic chain and the substituent in the 2-position of the tricyclic ring should be optimized to increase the binding affinity toward both RNA structures.

Since our experimental results confirmed our virtual screening prediction that acetopromazine would bind to two very different bulges such as the purine-rich A-site RNA and the previously studied pyrimidine-rich HIV-1 TAR RNA, we decided to ascertain whether the ligand binds to other RNA motifs as well. Three other RNA molecules with different characteristics that were available to us in the laboratory were chosen. All five RNA molecules that were tested for their interaction with acetopromazine are shown in Figure 6. They range in length from 18 to 38 nucleotides: (A) A-site rRNA; (B) HIV-1 TAR RNA; (C) coxsackie virus B3 RNA; (D) polio virus loop B RNA; (E) UUCG hairpin. Structures C and D occur in the 5′-untranslated regions of the polio virus and coxsackie virus B3 genomic RNAs. The 38mer coxsackievirus B3 loop D RNA consists of two internal bulges, one six-residue pyrimidine bulge and one asymmetric UA bulge.[29] The 19mer polio virus loop B structure contains a loop consisting of seven nucleotides. We also included a 18mer UUCG ultrastable tetraloop motif which was otherwise exclusively Watson−Crick base-paired as a putative negative control.

The 38mer RNA from loop D of the coxsackie virus B3 IRES site (Figure 6C) contains two internal bulges. One is a symmetric bulge consisting of six pyrimidines, and the second bulge is asymmetric containing sequential U and A residues. TOCSY spectra revealed pyrimidine H5, H6 chemical shifts larger than 0.03 ppm in both loops with an acetopromazine concentration of 0.6 mM. In the larger symmetric bulge, only the two central residues U12 and U29 showed shifts above our threshold of 0.03 ppm. The asymmetric UA bulge showed shifts in both the upper and lower stem closing base pair cytosines C4 and C34 as well as U5 located in the bulge. A small shift was observed for the C38 residue located at the closing base pair. We also monitored chemical shifts of the imino resonances. The affinity for the larger symmetric U-rich bulge could not be determined because the imino resonances of the wobble U11, U30, and the G31 base pairs only started shifting at concentrations of 0.5 mM or higher. From the chemical shift monitoring of the G35

(29) Du, Z.; Yu, J.; Andino, R.; James, T. L. *Biochemistry* **2003**, *42*, 4373−4383.

Table 2. Dissociation Constants K_D Determined from Chemical Shift Monitoring Experiments for the Five Studies of RNA Molecules

	residues	K_D (mM)
(a) A-site RNA	27	0.36
(b) HIV-1 TAR RNA	31	0.27
(c) CVB loop D RNA	38	0.33 (UA bulge)
(d) PV loop B RNA	19	1.80
(e) UUCG hairpin RNA	18	no binding

imino resonance, we determined a dissociation constant of 330 μM for the asymmetric UA bulge. The imino resonance for G7 was detected only for the free RNA; it disappeared completely at a 150 μM acetopromazine concentration so data could not be fit. We cannot determine whether acetopromazine in effect binds to both bulges or whether the binding only takes place in the UA bulge, and all we observe are indirect effects in the U-rich bulge. This is a possibility especially since the largest chemical shift in the U-rich bulge is five base pairs removed or ca. half a turn from the UA bulge. This places the binding site of the drug on the same side of the helix, which could lead to the observed effects. Once again the affinity is weak, but the specificity of acetopromazine is clearly directed toward the bulges and not toward the hairpin loop or the double-stranded regions of the RNA.

We further tested the drug against a 19mer RNA from the loop B of the poliovirus IRES site (Figure 6D). It consists of a double-stranded region with 5 base pairs, a 3′-AC dangling end and a loop with 7 nucleotides. The TOCSY data revealed that only residues U6 and U8 showed significant shifts above 0.03 ppm at a ligand concentration of 0.6 mM. No shifts in double-stranded regions are observed, and the interaction is confined to the larger, flexible loop. This showed that acetopromazine also binds to terminal loop regions, if they are large enough to accommodate the ligand. The affinity of the acetopromazine for the loop was determined from TOCSY titration experiments by monitoring the chemical shift of the H6 proton of U6. The dissociation constant was determined to be ca. 1.8 mM from these experiments; this corresponds to an affinity 6 times weaker than acetopromazine has for TAR RNA.

Since there was no evidence of the ligand binding to the very stable tetraloop motifs of the A-site RNA or the HIV-1 TAR RNA or to regular double-stranded RNA stretches, we studied the UUCG hairpin RNA (Figure 6E), which served as a negative control. It contained solely a UUCG-tetraloop and Watson−Crick base paired regions to test the specificity of phenothiazines for non-double-stranded RNA motifs. In this case both NOESY and TOCSY spectra were acquired and no chemical shift changes other than those of the closing base pair G1 and C18 were observed. One possible cause for the binding to the closing base pair could be the increased flexibility; stacking of the aromatic rings on the terminal base pair is also possible and seems more likely since shifts were not observed on polio virus loop B with the dangling AC bases. Lack of ligand resonances in the STD NMR spectra, no trNOESY cross-peaks, and no observable line broadening also prove that the ligand binds extremely weakly at best.

Table 2 summarizes the results of the binding interactions of acetopromazine and the five RNA molecules studied. The strongest interaction of the acetopromazine is observed for the TAR RNA, A-site RNA, and the CVB loop D RNA structures

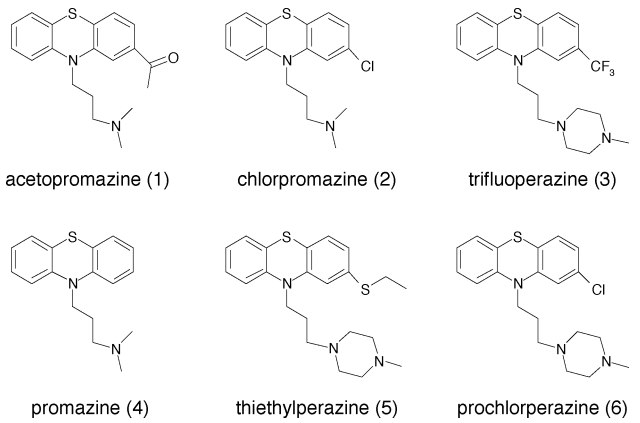

Figure 8. Commercially available phenothiazines tested for their interaction with the A-site ribosomal RNA. The affinity of the tested compounds was characterized by the STD NMR intensity and the degree of line broadening at similar RNA−ligand ratios. The affinity toward the A-site RNA decreases from compound **1** to **6**.

with K_D values of 270, 360, and 330 μM, respectively. The polio virus loop B showed a very weak affinity of 1.8 mM with the acetopromazine ligand. No affinity could be calculated for the larger symmetric loop of the CVB3 loop D because the slope of the concentration plotted versus the chemical shift was still linear up to 1.5 mM acetopromazine which lead to our estimate of $K_D > 3$ mM. The UUCG tetraloop showed only very small chemical shifts of the closing base pair in the TOCSY spectrum and therefore effectively served as a negative control.

Acetopromazine apparently has a slight preference for smaller bulges consisting of two or three unpaired bases. Larger loops or bulges, i.e., the 7-nucleotide loop of the polio virus loop B ($K_D = 1.8$ mM) and the symmetric U-rich bulge of the CVB loop D consisting of six bases ($K_D > 3$ mM), decreased the interaction by a factor of 6 or more compared to bulges of the A-site and TAR RNA structures. There is also no obvious preference for purine versus pyrimidine residues. Another open question is whether an adaptive RNA binding site has advantages over a very rigid RNA motif in terms of binding affinity. The answer would be of general interest and not only for the acetopromazine RNA system studied here.

Phenothiazine Derivatives Binding to A-Site RNA. To further characterize the binding interaction, five other commercially available phenothiazine derivatives were tested against the ribosomal A-site RNA (Figure 6A). All six compounds shown in Figure 8 bound to the A-site RNA, however, with different affinities. Classification was conducted by studying the STD intensities and monitoring the degree of line broadening of the compounds at identical ligand-to-RNA ratios and concentrations. In all cases, the highest STD intensities were observed for the aromatic region of the six compounds with intensities ranging from 80% at 10-fold ligand excess for compound **1** to 10% for compound **6**. In addition, the degree of line broadening agreed with the rankings from the STD experiments. Stronger line broadening at the same ligand excess indicated higher affinity, i.e., compounds **4**−**6** showed very little line broadening whereas resonances of compounds **1**−**3** broadened considerably upon addition of A-site RNA.

To corroborate our classification of the binding affinity, we titrated compound **4** into a H_2O sample of A-site RNA and again monitored the imino proton chemical shift changes. No imino resonance shifts were detected up to a ligand concentration of

0.5 mM under conditions identical to the first titration displayed in Figure 5. And even at a 1 mM concentration of compound **4**, only imino resonances of the U5, U23 wobble base pair shifted by 10 Hz. This proves that compound **4** has a much weaker affinity toward the A-site RNA as predicted by the STD and line broadening experiments.

Six compounds are not enough to deduce a SAR. However, some preferences become evident. The acetyl and chloro derivatives in the 2-position improve the binding affinity compared to the unsubstituted phenothiazine, compound **4**. The *N*-piperidino group on the side chain also markedly reduces the affinity of the 2-chloro derivative as can be observed for compound **6**. It would be interesting to synthesize and test whether the trifluoromethyl derivative (compound **3**) in combination with the aliphatic *N*-dimethylpropylamino side chain would lead to a higher affinity compound since the binding affinity of compound **3** is higher than that of compound **6**. As can be seen for compound **5**, a thiethyl substitution in combination with the *N*-piperidino group also reduces the affinity. This preliminary data shows that the binding affinity of the A-site RNA is responsive to ligand characteristics and that the affinity can be modulated by addition or deletion of certain chemical groups. This gives hope that eventually this scaffold can be fine-tuned to bind to a variety of unique tertiary RNA structures with the required affinity and specificity. In the relatively new field of targeting RNA with small molecules, it remains to be seen if one will be able to generate a drug of high affinity and specificity from a low affinity lead compound as has been accomplished for protein targets. In this regard, it was recently shown that an affinity increase of an A-site ligand by a factor of 50 can be accomplished by relatively small chemical modifications.[27] The lack of ideal druglike small molecules binding to RNA makes the phenothiazine scaffold a very interesting candidate.

In conclusion, the first four RNAs studied interacted specifically with the ligand. In each case, the ligand showed binding to either the internal bulges of the RNA, or the apical loop region, as seen for the polio virus loop B which contained more than seven nucleotides. Binding to regular double-stranded RNA regions or tetraloop motifs was not observed even at 10- to 20-fold ligand excess. We also showed that acetopromazine has different affinities for the five different RNA molecules studied with the K_D ranging from 270 μM for the TAR RNA to greater than ca. 3 mM for the U-rich bulge of the CVB3 loop D RNA. Phenothiazines are a novel nonnucleotide, nonpeptide scaffold for RNA binding drugs. Their propensity to exclusively bind to the most interesting RNA regions, from the perspective of specificity, combined with their low toxicity and high bioavailability makes them ideal as a scaffold. However, the relatively low affinity of these compounds will need to be improved drastically for the respective RNA motifs for them to be used as drugs. Fine-tuning of the affinity could go hand in hand with gaining specificity for the respective target RNA structure. Lead compounds with comparable affinity for targeted proteins have subsequently been engineered to bind with nanomolar affinity.

Acknowledgment. This work has been supported by a fellowship to M.M. from the German Academic Exchange Program (DAAD) and by NIH Grant AI46967. We are grateful for RNA samples provided by Drs. Jinghua Yu, Zhihua Du, and Anwer Mujeeb.

JA0398870